Interference between direct and resonant channels in near-resonance photoemission in argon

R. R. T. Marinho,[1] O. Björneholm,[2] S. L. Sorensen,[3] I. Hjelte,[2] S. Sundin,[2] M. Bässler,[2] S. Svensson,[2] and A. Naves de Brito[1,4,*]

[1]*Institute of Physics, Brasilia University, 70 910 900 Brasilia DF, Brazil*

[2]*Department of Physics, Uppsala University, Box 530, S-751 21 Uppsala, Sweden*

[3]*Department of Synchrotron Radiation Research, Institute of Physics, University of Lund, S-221 00 Lund, Sweden*

[4]*Laboratório Nacional de Luz Sincrotron, Box 6192, CEP 13083-970 Campinas SP, Brazil*

(Received 27 June 2000; published 13 February 2001)

The wave nature of electrons, epitomized by Young's two-slit experiment, is also demonstrated in resonant photoemission. We present photoelectron spectra of argon measured in the vicinity of the $2p_{3/2}\rightarrow 4s$ core excitation. Interference effects are monitored by following the intensity of final states populated through both the resonant and the direct channel. The partial-electron-yield spectra of $3p^{-2}nd$ final states exhibit a rich variety of interference effects. This demonstrates the need for a unified one-step description of the ionization through a direct and a core-excitation mediated channel.

DOI: 10.1103/PhysRevA.63.032514 PACS number(s): 32.70.−n

The study of interference and coherence phenomena in atoms and molecules has resulted in the discovery of a number of fundamental effects where the lifetime width of the core hole is comparable to other involved energy scales [1,2]. A theoretical framework for a unified one-step treatment of the complete photoionization process, including direct and resonant channels, has been developed [1]. Due to its generality, however, less sophisticated theories have often been used in specific cases with reasonable success. The criteria for interference include coherent excitation, nonzero overlap of decay-channel wave functions, and comparable intensities of competing pathways. Studies of resonant processes involving core-electron excitation and decay in atoms and molecules [3], where a two-step nonunified model is often sufficient, laid the foundation for studies in a number of atoms [4–8]. The process of resonant core excitation and decay results in the same final states as direct photoemission. In analogy to the two-slit experiment, the direct and resonant channels could thus play the roles of the two pathways from the initial to the final state, making interference between the two possible. Interference implies a connection between the excitation and decay processes, and consequently evidence for interference implies a need for a one-step picture of the photoionization process. Recent studies of Ni metal have revealed interference effects in the vicinity of core thresholds [9]. The first observations of interference effects for the argon case were described by Camilloni *et al.* [8]. As we will show, the case at hand exhibits much more pronounced and varied interference effects. The combined resonant core excitation and decay process is often called resonant photoemission. This is a useful tool for the study of electronic structure of atomic matter. This is partly due to the selectivity of the core excitation, which has been utilized in systems where it is important to separate contributions from different types of atoms [10]. An additional strength lies in the ability to study femtosecond dynamics in condensed systems [10–13].

Still, these fundamental phenomena are manifested in their purest form in atomic systems, where a detailed understanding is crucial for extrapolation to more complex systems. An example is electronic state-lifetime interference [5,7,8]. Valence single-hole final states, which exhibit asymmetrical line profiles, have been measured in neon and argon and described within an interference picture [14]. Related asymmetric resonance features in core-level absorption in argon have been suggested by theory [15]; using the close-coupling approximation, the authors of Ref. [15] could accurately reproduce the effects of interference for the line shapes of the single-hole final states.

The object of the present study is the decay of the core-excited $2p_{3/2}^{-1}4s$ state in argon. The 2-eV spacing of electronic states in the absorption spectrum is large compared to the lifetime broadening ($\approx$0.1 eV) and the photon-energy bandwidth ($<$0.1 eV). Thus electronic state-lifetime interference may be neglected. The Ar $2p_{3/2}\rightarrow 4s$ resonance is experimentally attractive, being easily accessible with high intensity and resolution and the final states for on and off resonance excitation are thoroughly studied [14,16–18]. In this paper we present an experimental photoemission investigation of the $3p^4nl$ two-hole one-particle ($2h1p$) inner-valence states in argon at photon energies near the $2p_{3/2}\rightarrow 4s$ resonance. Because of the relatively weak direct photoabsorption cross section, the resonant channel is dominant on resonance. We find, however, that a slight detuning from the resonance maximum leads to striking changes in the populations of these final states. We attribute these effects to interference. The range of interference effects is seen to extend quite far outside the resonant region.

The experiments were performed at the I411 beam line at MAX-LAB, the Swedish national synchrotron radiation laboratory [19]. The photon-energy resolution was 70 meV. Resonant photoemission spectra were recorded with an electron kinetic energy resolution of 75 meV at the ''magic'' angle 54.7° between the photon polarization and electron emission directions to avoid angular discrimination effects. The Ar gas was commercially obtained (Air Liquide) with a purity of 99.999%.

*Email address: arnaldo@lnls.br

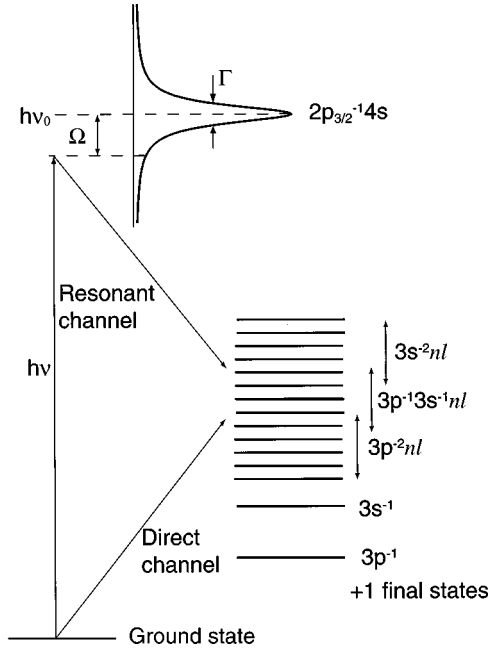

FIG. 1. A schematic representation of the involved states, as well as the direct and resonant channels.

To discuss resonant photoemission, it is appropriate to start with the electronic states and transitions involved. The processes involved in this study are schematically shown in Fig. 1. The lowest ionic states of argon are single hole ($1h$) states, $3p^{-1}$ or $3s^{-1}$. At higher energies a multitude of $2h1p$ states, belonging to the $3p^{-2}nl$, $3p^{-1}3s^{-1}nl$, or $3s^{-2}nl$ manifolds, are found. In direct, nonresonant photoemission, the $1h$ states are strongly dominant, and the $2h1p$ states are observed as weak satellites [14]. The direct channel can be considered to be the only channel for photon energies far from any core excitation energy. For photon energies corresponding to the core excitation energies, however, there is also a resonant, core-hole mediated, channel. The lowest core-excited state, $2p_{3/2}^{-1}4s$, is situated 244.34 eV above the ground state, and has a natural lifetime broadening Γ of 114 ± 2 meV [20]. There exist several other core-excited states above this, but as they are separated from $2p_{3/2}^{-1}4s$ by more than 2 eV, they may presently be neglected. The main features in the resonant decay spectrum are $2h1p$ states due to spectator decay [5,21], which are well described within the strict spectator model [16] and the shake-modified spectator picture [22]. The resonant enhancement of $1h$ final states though participator decay was determined in this study to be less than 5%. This is in accord with recent theoretical predictions, where no resonant enhancement was predicted for the $3p_{1/2}^{-1}$ cross section [15].

The photoemission spectra of the $2h1p$ states in the $3p^{-2}nl$ region recorded for three different photon energies near the $2p_{3/2}\rightarrow4s$ resonance energy are shown in Fig. 2. The detuning Ω is defined as the difference between the resonance energy $h\nu_0$ (i.e., the energy of the $2p_{3/2}\rightarrow4s$ resonance) and the photon energy $h\nu$. The spectra represent three distinct cases: far below resonance ($\Omega=-7.5$ eV), where practically only the direct channel contributes, on

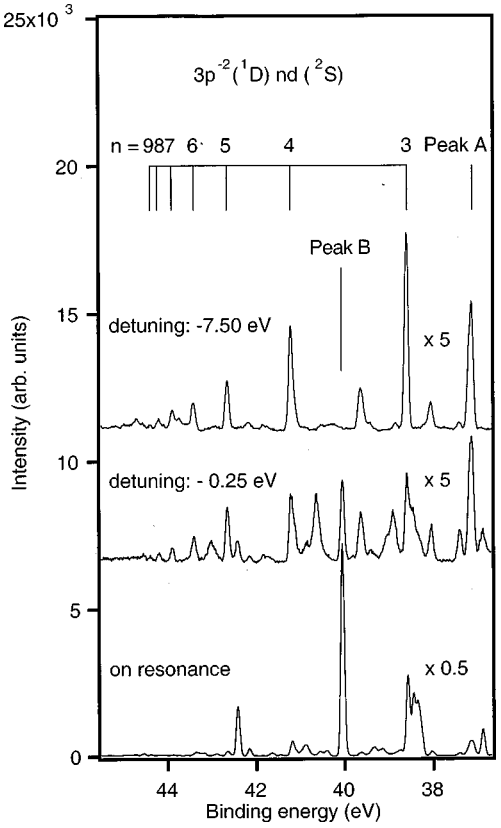

FIG. 2. The photoemission spectra of the $(3s,3p)^{-2}nl$ region recorded after excitation with detunings 0.00, -0.25, and -0.75 eV relative to the $2p_{3/2}^{-1}4s$ resonance energy. The spectra were normalized to the $3p_{1/2}^{-1}$ intensity.

resonance ($\Omega=0.00$ eV), which is almost completely dominated by the resonant channel, and an intermediate case just below resonance ($\Omega=-0.25$ eV). Assignments of the main spectral peaks can be found in Table I. Since the spectra cover the range from off resonance to on resonance, the intensities differ radically from spectrum to spectrum. Most of the states that have high intensity in the on-resonance spectrum are $2h1p$ states with a $3p^{-2}(^1D)ns(^2D)$ configuration. The configurations of the strongest off-resonance peaks include both $3p^{-2}(^1D)nd(^2D)$ and $3p^{-2}(^1D)nd(^2S)$ states. Members of the latter series, which is characterized by the same core and valence coupling but differing main quantum number of the *d* Rydberg electron, are indicated in Fig. 2. The relative importance of the direct and resonant channels is strongly photon-energy dependent: whereas the direct channel to a good approximation may be considered to have constant cross section in the small energy interval considered here, the cross section of the resonant channel depends on where in the Lorentzian-shaped resonance the excitation is done.

Can the near-resonance spectra be understood as properly weighted superpositions of the direct and resonant spectra? To investigate this, let us consider the two peaks labeled *A* and 3 in Fig. 2. The *A* peak contains the close-lying $3p^{-2}(^1D)3d(^2D)$ and $3p^{-2}(^1D)4p(^2P)$ states. The 3 peak corresponds to the $n=3$, $3p^{-2}(^1D)nd(^2S)$, Rydberg series mentioned in the previous paragraph. Both in the on-

TABLE I. Assignment and Fano parameters of some selected final states [28]. The assignments are taken from [6,14,16,17].

Peak	Binding energy (eV)	Assignment	Max. intensity relative to $3p_{1/2}^{-1}$ peak	Position of max. intensity relative to $h\nu_s$	q	σ_T	Γ (meV) [26]	ρ
Total ion yield		$2p_{3/2}4s$		0.00	1.3×10^2	49.01	106(5)	0.16
A	37.112	$3p^4(^1D)4p^1(^2P)\ J=\frac{3}{2}$ $3p^4(^1D)3d^1(^2D)\ J=\frac{5}{2}$	0.01	−0.06	1.2×10^1	0.103	155(15)	0.08
B	40.054	$3p^4(^1D)5s^1(^2D)$ $3p^4(^3P)4f$	1.39	−0.03	8.2×10^2	0.002	100(5)	0.09
$3d$	38.570	$3p^4(^1D)3d^1(^2S)\ J=\frac{1}{2}$	0.48	0.00	3.5	0.049	137(5)	1.71
$4d$	41.208	$3p^4(^1D)4d^1(^2S)\ J=\frac{1}{2}$	0.09	0.06	1.2	0.023	116(5)	2.42
$5d$	42.659	$3p^4(^1D)5d^1(^2S)\ J=\frac{1}{2}$	0.05	−0.06	−1.3	0.005	86(5)	3.89
$6d$	43.427	$3p^4(^1D)6d^1(^2S)\ J=\frac{1}{2}$	0.02	0.06	0.6	0.003	110(5)	3.91
$7d$	43.911	$3p^4(^1D)7d^1(^2S)\ J=\frac{1}{2}$	0.01	−0.18	−0.1	0.003	110(5)	2.48

resonance and off-resonance spectra the 3 peak is stronger than the *A* peak. In the intermediate spectrum, however, the relative intensity is reversed. The variations of relative intensity as function of detuning energy are thus not monotonic, demonstrating that the near-resonance spectra cannot be described as simple superpositions of the direct and resonant spectra. The observed behavior is instead indicative of interference between the direct and resonant channels.

In order to quantitatively study this interference, the individual peaks in spectra recorded at 21 photon energies around the $2p_{3/2}\rightarrow4s$ resonance were fit using Voigt profiles of average width 0.110 eV. The peak intensities for each photon energy were scaled according to the intensity of the $3p_{1/2}^{-1}$ peak. The energies and widths obtained from a free fit agree well with previously published data [6,14,16,17]. In subsequent fits the shape and binding energy of all peaks were kept fixed.

The development of several final states through the $2p_{3/2}\rightarrow4s$ resonance region is shown in Fig. 3 together with the absorption spectrum [23]. Before continuing to the strong interference cases, it should be mentioned that most final states are not heavily influenced by interference. The partial electron yields of such states follow the absorption cross section very closely. An example of this behavior is the $3p^4(^1D)5s^1(^2D)$ state that dominates the peak labeled *B* in Fig. 3. In the subsequent frames, the partial yields of the $3p^4(^1D)nd(^2S)$ Rydberg series are shown. In contrast to the *B* case, these do not follow the absorption cross section.

The partial yield of ''$3d$'' differs slightly from $2p_{3/2}\rightarrow4s$ absorption; the maximum is at the same energy, but it exhibits a pronounced asymmetry. The difference for peaks of higher n is more striking. Apart from the intensity maxima, they also display clear intensity minima. The maxima and minima are shifted away from the $2p_{3/2}\rightarrow4s$ absorption maximum, and the asymmetry thus produced changes dramatically as a function of n. The ''$7d$'' does not exhibit even a clear maximum, but only a clear minimum. We find this to be a very rich and varied resonance behavior, which we attribute to interference between the direct and resonant channels.

The original theory developed by Fano [25] was limited by the assumption that each discrete level is completely iso-

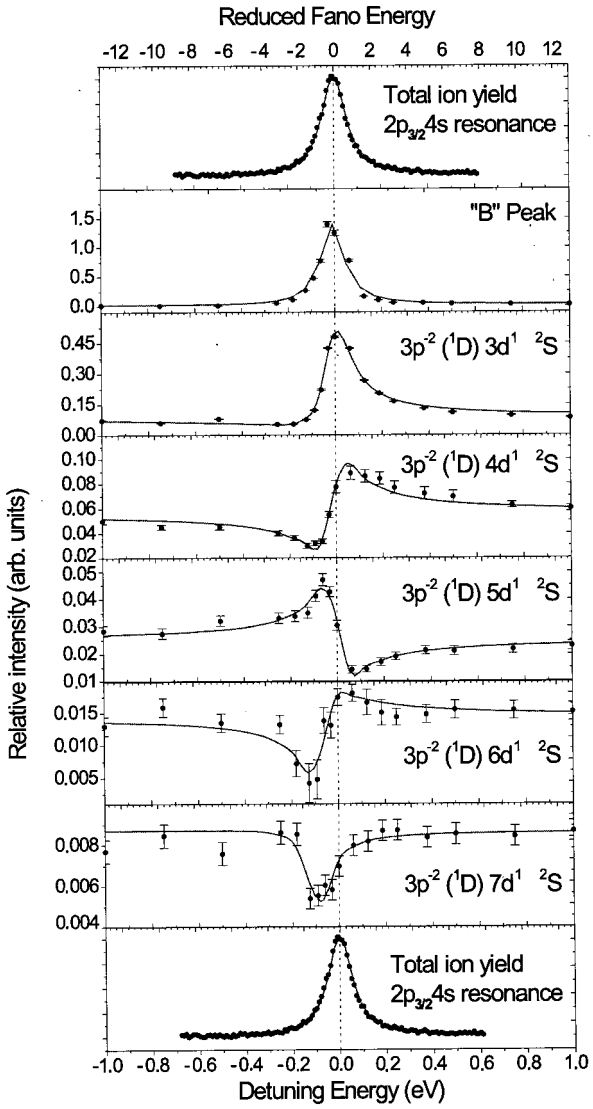

FIG. 3. The intensities of some selected final states in the vicinity of the $2p_{3/2}^{-1}4s$ resonance energy at $\Omega=0$ (marked by a vertical line). The intensities are relative to the $3p_{1/2}^{-1}$ intensity, which is approximately 0.6 Mbarn [24], and varies less than $\pm5\%$ in the investigated photon-energy interval.

lated from other levels. In principle, this limitation excludes the use of the formalism in the present situation where several Rydberg series are overlapping, and where the extent of the interference extends several eV below the resonance. Fano and Cooper developed an extension of the original theory in which this interaction is represented by a correlation parameter in addition to the familiar Fano asymmetry parameter [26]. The original Fano formalism for interference between a discrete and continuum state is thus not strictly applicable to this case but has been shown to be valid in many cases despite the existence of a coupled term and in the correlation parameter for partial cross section. We follow the formalism developed by Fano and Cooper as a useful framework for analyzing the data. Taking the finite bandpass $\Delta h\nu$ of the exciting photons into account, the cross section for a certain final state as function of the photon energy $h\nu$ may then be written as [27]

$$\sigma(h\nu)=\sigma_T\left\{\rho'^2\left[\frac{(q+\varepsilon')^2}{\varepsilon'^2+1}+\frac{\Delta h\nu}{\Gamma}-1\right]+1\right\}.$$

Here σ_T is proportional to the strength of the direct channel well off-resonance, Γ is the width of the partial electron yield channel, and ρ' is the modified correlation coefficient between decay channels. The reduced Fano energy ε is defined as $\varepsilon=2\Omega/\Gamma$ and for a finite bandwidth $\varepsilon'=\varepsilon(1+\Delta h\nu/\Gamma)^{-1}$ and the modified correlation coefficient is defined likewise as $\rho'=\rho(1+\Delta h\nu/\Gamma)^{-1}$. The interference parameter q is connected to the relative amplitudes and phases of the two channels. For large q, the line shape approaches a Lorentzian. A small value of q corresponds to strongly non-Lorentzian asymmetric line shapes with a dip below ($q>0$) or above ($q<0$) $h\nu_0$ as well as a shift of the maximum intensity away from $h\nu_0$. This q parameter is most directly connected to the strength of the interference and a small q value is indicative of such effects.

We have fit the resonance profiles in Fig. 3 to the Fano profile and extracted Γ, q, σ_T, and ρ, see Table I. The fits are displayed as solid curves. The behavior of the $3d$ peak, characterized by a q of approximately 3.51, is only moderately affected by interference. It has a weak minimum below $h\nu_0$, and a clearly asymmetric non-Lorentzian line shape. A more pronounced example is found in the ''$4d$'' peak, with a smaller q of approximately 1.22. This exhibits a minimum before $h\nu_0$ followed by a maximum above $h\nu_0$. This behavior is reversed in the ''$5d$'' profile. With $q=-1.27$, this instead shows a minimum caused by destructive interference above $h\nu_0$. ''$6d$'' is qualitatively similar to $4d$. Another type of resonance profile is exhibited by the $7d$ with a q of -0.11. This has no clear maximum, but only a minimum. This reduction of the cross section is due to destructive interference, and ''$7d$'' is an example of a ''window'' resonance. Its resonance behavior is in some sense opposite to that of $3d$.

The members of the Rydberg series exhibit diverse behavior, ranging from strongly resonant to strongly antiresonant. To our knowledge, this is the first time that strong evidence of Fano behavior has been observed for partial core photoionization cross sections in free atoms. This type of behavior should be present in many other systems, including molecules, surfaces and solids, and should be kept in mind when using resonant photoemission to study the electronic structure, or when nontotal electron yield is used for studies of x-ray absorption.

In conclusion, the partial electron yields of $3p^4(^1D)nd(^2S)$ states in argon have been studied in the $2p_{3/2}\rightarrow 4s$ resonance region. We observe clear interference effects in the partial yields as a function of photon-energy detuning. The interference is between direct photoemission and resonant photoemission via the $2p_{3/2}^{-1}4s$ resonant core-excited state. Surprising changes in the resonance profiles are found through the progression of final states, which were analyzed using the Fano formalism for interference between a discrete and continuum state. A detailed understanding of this rich variation of the resonant profiles constitutes a challenge to theory. The results clearly demonstrate the need for a one-step description of the ionization process unifying the direct and resonant channels.

This work has been supported by the Swedish Foundation for International Cooperation in Research and Higher Education (STINT), the Swedish Natural Research Council (NFR), and National Council for Scientific and Technological Development (CNPq Brazil). M.B. acknowledges the support from Swedish Foundation for Strategic Research (SSF), through a Senior Individual Grant and Swedish Research Council for Engineering Sciences (TFR).

[1] T. Åberg, Phys. Scr., T **41**, 71 (1992).
[2] C.-O. Almbladh and L. Hedin, in *Handbook on Synchrotron Radiation*, edited by E.-E. Koch (North-Holland, Amsterdam, 1983), Vol. 1B.
[3] M. O. Krause *et al.*, J. Phys. (Paris) **32**, C4-139 (1971).
[4] J. A. de Gouw *et al.*, J. Phys. B **28**, 2127 (1995).
[5] J. A. de Gouw *et al.*, J. Phys. B **28**, 1761 (1995).
[6] J. A. de Gouw *et al.*, J. Phys. B **25**, 2007 (1992).
[7] J.-E. Rubensson *et al.*, Chem. Phys. Lett. **257**, 447 (1996).
[8] R. Camilloni *et al.*, Phys. Rev. Lett. **77**, 2646 (1996).
[9] M. Weinelt *et al.*, Phys. Rev. Lett. **78**, 967 (1997).
[10] *Applications of Synchrotron Radiation*, edited by W. Eberhardt (Springer-Verlag, Berlin, 1995).
[11] A. Sandell *et al.*, Phys. Rev. Lett. **78**, 4994 (1997).
[12] O. Karis *et al.*, Phys. Rev. Lett. **76**, 1380 (1996).
[13] C. Keller *et al.*, Phys. Rev. Lett. **80**, 1774 (1998).
[14] A. Kikas *et al.*, J. Electron Spectrosc. Relat. Phenom. **77**, 241 (1996).
[15] T. W. Gorczyca and F. Robicheaux, Phys. Rev. A **60**, 1216 (1999).
[16] M. Meyer *et al.*, J. Electron Spectrosc. Relat. Phenom. **51**, 407 (1990).

[17] H. Aksela and J. Mursu, Phys. Rev. A **54**, 2882 (1996), and references therein.
[18] J. Mursu *et al.*, J. Phys. B **29**, 4387 (1996).
[19] M. Bässler *et al.*, J. Electron Spectrosc. Relat. Phenom. **101–103**, 953 (1999).
[20] O.-P. Sairanen *et al.*, Phys. Rev. A **54**, 2834 (1996).
[21] M. Meyer *et al.*, Phys. Rev. A **49**, 3685 (1994).
[22] B. Langer *et al.*, J. Phys. B **30**, 4255 (1997).
[23] The error bars indicate the intensity uncertainty, determined as a propagated error derived from the square root of the number of counts plus a contribution estimated from the varying results of different fitting strategies.
[24] J. J. Yeh and I. Lindau, At. Data Nucl. Data Tables **32**, 1 (1985).
[25] U. Fano, Phys. Rev. **124**, 1866 (1961).
[26] U. Fano and J. W. Cooper, Phys. Rev. A **137**, A1364 (1965).
[27] S. L. Sorensen *et al.*, Phys. Rev. A **50**, 1218 (1994).
[28] For the $2p_{3/2}^{-1}4s$ state, the Γ determined by the Fano formalism (106 meV) differs slightly from that obtained by fitting with a Voigt function (114 meV). We attribute this discrepancy to a tendency of the presently used Fano profile to slightly underestimate the width for the ''pure'' Lorentzian shape. We do not claim that Γ of the $2p_{3/2}^{-1}4s$ state is 106 meV, but the value is there to give the reader a precise idea of what the present Fano formula gives as width for a known profile.